

NASA DEVELOP National Program



BLM at Idaho State University GIS TReC
Fall 2016

Southeastern Idaho Water Resources Leveraging NASA Earth Observations to Identify Existing Surface Water Features and Improve Water Management and Resource Allocation in Southeastern Idaho

DEVELOP Technical Report Final Draft – November 17, 2016

Traci Olson (Project Lead)
Cody O'Dale
Dylan Thomas
Caitlin Toner
Courtney Ohr

Keith Weber, Lead Science Advisor (GIS Training and Research Center at Idaho State University)
Mark Carroll (NASA GSFC)
Charles Peterson (Biology Department, Idaho State University)

1. Abstract

Understanding water dynamics in southeastern Idaho is critical to planning and improving water management practices. Partner organizations that focus on water management, such as the Bureau of Land Management (BLM) and Idaho Department of Water Resources (IDWR), use national hydrography dataset product and legacy knowledge to identify water bodies. However, this approach has been insufficient to meet all their needs. This can lead to ineffective use of resources and may put sensitive species at risk, while allowing invasive species to thrive. This study uses NASA Earth Observations and Google Earth Engine to create a tool that allows end-users to better identify and track water bodies within their management area. The Surface Water Indicator Model (SWIM) tool incorporates multiple water indices, and topographic data into a classifier. Common features including mountain shadows, urban asphalt, basaltic lava flows, or dark vegetation are often confused with water in automated detection algorithms. This study combines multiple methods into a single tool to create a more accurate indicator of surface water. The resulting SWIM tool is user friendly allows surface water indication with the most currently available Landsat 8 imagery, and can be used to monitor temporal changes in surface water. The tool was developed within Google Earth Engine (GEE) and a parallel model in ArcGIS using Python. This duplication gives the end-user a choice of platform that best fits their needs. The SWIM tool will help natural resource managers with project planning, field assignments, and allocation of resources.

Keywords

Remote sensing, surface water, Support Vector Machine, Landsat, water index, water resources, SWIM, Google Earth Engine.

2. Introduction

2.1 Background Information

Previous research has identified water bodies through the use of water indices (McFeeters, 2013) or a classification algorithm (Wright & Gallant, 2007), but most have not combined the two methods. Often, any one of these methods alone will incorrectly identify water from features like mountain shadows (Jin et al. 2013), urban asphalt (Feyisa et al. 2014), basaltic lava flows, or dark vegetation (Jawak et al. 2015). This study combines multiple water indices and a classification algorithm into a single tool to create a more accurate surface water indicator that takes advantage of Landsat's extensive record of earth observation imagery. The study area for this project was southeast Idaho demarcated by the Eastern Idaho Bureau of Land Management (BLM). The scope of this study area included the east edge of Craters of the Moon National Monument to the southeast corner of Idaho. The landscape hosts abundant ecological variability including large areas of basaltic lava flows, forested mountains, marshlands, reservoirs, ponds, rivers, and large areas of sporadic vegetation with bare soil. This study used Landsat 8 imagery from late June 2016 for its initial testing, but was designed for broader partner use as a seasonal water monitoring tool.

monitor changes in water resources. These changes may be driven by availability of snowpack/precipitation or they could be the result of seasonal variation.

2.3 Classifiers

2.3.1 Support Vector Machine (SVM) Classifier

A Support Vector Machine (SVM) classifier is a supervised machine-learning algorithm that helps describe, categorize, and generalize a particular dataset. This algorithm was originally developed for pattern recognition and is commonly used for image classification because of its strong theoretical foundation and experienced success (Cafarella et al. 2008). SVM aims to find the uniform convergence or the “true” mean of spectral signatures of the labeled training points. This creates a division line or classifier with the largest gap between the classifier and the training data, which is called trick optimization (Figure 2A). When the unlabeled pixel signatures are plotted on the chart they will fall on either side of these class lines giving the predicted classification. SVM can also create hyperplanes when signatures become more complex and there is no way to create a simple line for the mean of a signature class (Figure 2B). Creating a hyperplane involves kernelling or transforming the data so that it becomes more uniform and then the hyperplane is drawn so that three dimension or three variables are considered (Burges, 1998). Normally, using SVM results in decreased computation time and increased memory requirements; however, a parallel SVM algorithm was implemented within Google Earth Engine (GEE) due to its memory capacity which bypassed these downfalls. There is not a similarly adapted algorithm within ArcMap. Nevertheless, users can define the number of processors used for the SVM computation which does help negate some of the computation complexities.

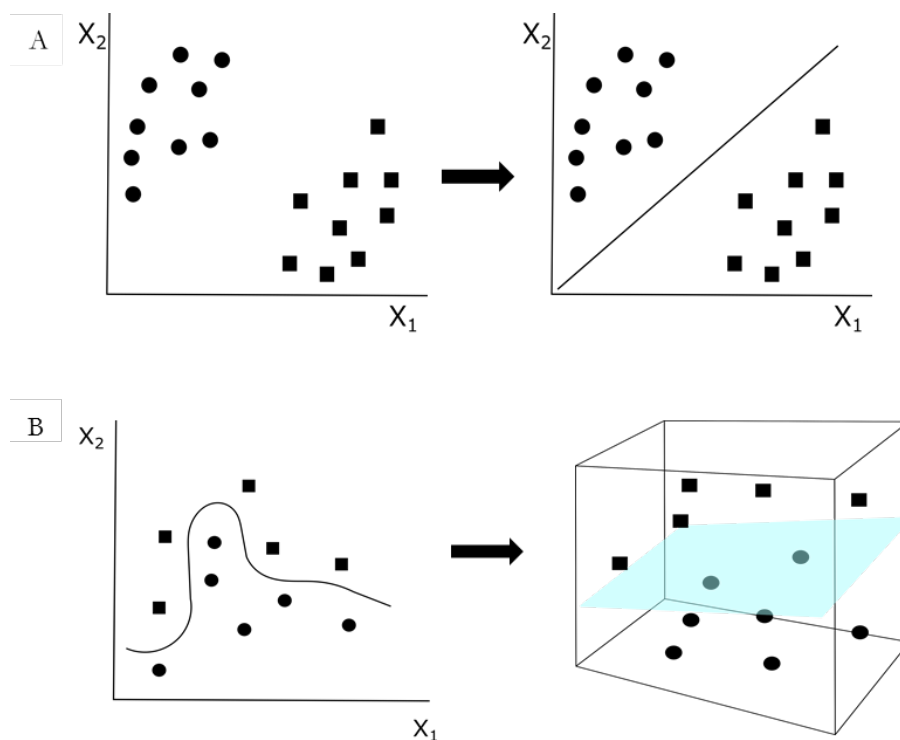


Figure 2 Classifying with SVM where two classes (shown as circles for water and squares for non-water) are known to be present. A) The mean is shown with the line and has been trick optimized so that the distances from the closest point in each of the two groups will be farthest away. Wherever the unlabeled signatures fall will decide if it is water or not water. B) When the labeled training data has too much variation a transformation is implemented and a hyperplane (shown in blue) is created

2.3.2 Classification and Regression Tree (CART) classifier

A Classification and Regression Tree is a machine-learning algorithm that helps describe, categorize, and generalize a particular dataset (Brieman et al. 1984). The Classification and Regression Tree is a predictive modeling machine that uses tree algorithms to find a target value or variable.

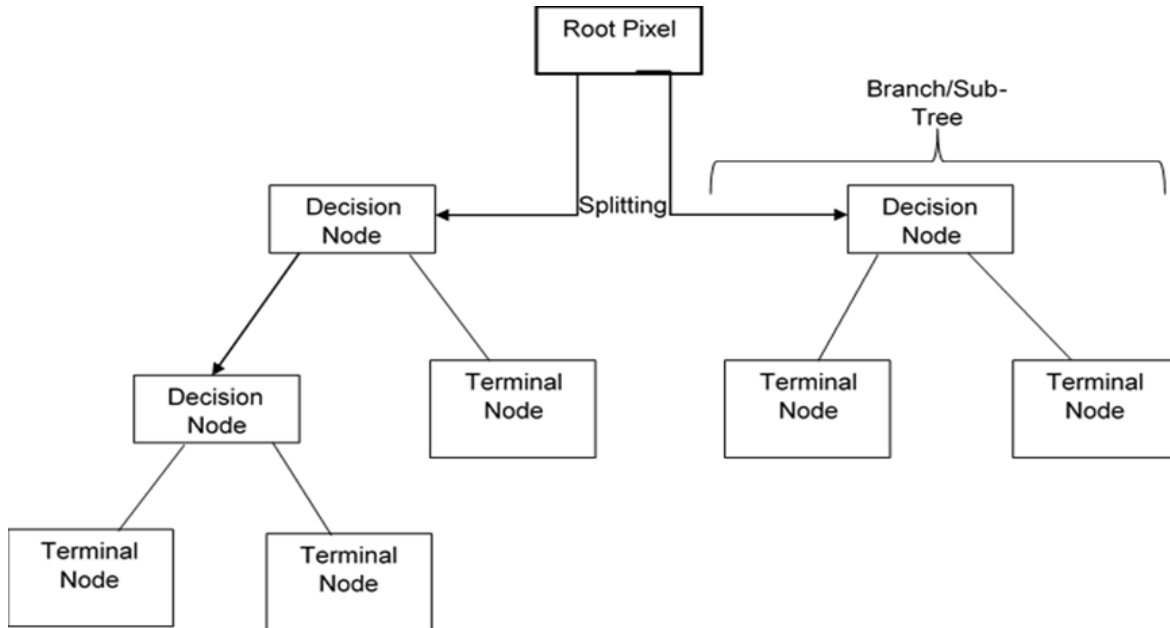


Figure 3 A visualization of CART decision tree.

2.4 Hosting Platforms: Google Earth Engine (GEE) & Esri ArcGIS

Two platforms were used to host the SWIM tool, this increased usability across multiple audiences. For instance, more technology advanced users have the ability to customize the model with GEE while Esri's ArcMap provides accessibility for users who are already familiar with the Esri programs. GEE is an internet cloud-based geospatial platform that processes satellite imagery and other global observation data. This platform integrates a variety of available public datasets and uses Google's server capacity to perform a plethora of geospatial processing. The result of this powerful computation easily allows users to search, sort, apply, and analyze datasets inside Google's infrastructure. Landsat 8 and other image collections can be seamlessly called into a map and filtered through many types of calibrations. Additionally, work done on GEE can be integrated into a publicly available console and thus, shared with other users. A downfall of this platform is the script based interface instead of a more common Graphical User Interface (GUI). This requires users to make JavaScript based edits to use SWIM in GEE. A GUI may be more intuitive, but a script based interface enables a higher degree of modification. This type of platform will require a detailed guided tutorial to acquaint users with parts of the program that may not be intuitive. GEE's guide and the GEE community offer further assistance with the program's operability.

The Esri software suite provides multiple platforms for visualizing, analyzing, and exploring spatial relationships, patterns and trends. While this suite is tailored toward vector data rather than raster processing, the software is widely used and therefore ideal for disseminating the SWIM tool. The Esri ArcMap software allows production of a GUI providing a more intuitive interface for users unfamiliar with programming technology. The creation of a GUI will require less intense tutorials however, the overall ability of the SWIM tool may vary from the GEE developed SWIM tool due to available classifiers and computation performance differences across the two platforms.

2.5 USGS Dynamic Surface Water Extent product (DSWE)

The U.S. Geological Survey (USGS) is in the process of creating the Dynamic Surface Water Extent (DSWE) product with the aim of providing increased spatial and temporal monitoring of the dynamics of non-ocean surface water extents (Jones & Starbuck, 2015). These products are being produced to include the entire archived and currently available Landsat imagery. An early look at water indices, as well as the provisional Dynamic Surface Water Extent (DSWE) from the U.S. Geological Survey, did seem to indicate that basaltic rock often gave false water signatures (Jones & Starbuck, 2015). This could be problematic since, it is common to find large basalt formations and smaller rock outcrops in southeastern Idaho.

3. Methodology

The SWIM tool consists of three types of inputs: water indices, topographic layers, and secondary variables, derived from Landsat 8 Operational Land Imager (OLI), Thermal Infrared Sensor (TIRS), or from Shuttle Radar Topography Mission (SRTM) data. These components were all used within a supervised classifier called a Support Vector Machine (SVM) (Cortes & Vapnik, 1995). The SVM classifier was compared to CART classifier. Training points were used by the SVM to distinguish commonalities of each class, and label such signatures as water bodies or common non-water features. Over 400 training points were specified for each of the six classes: basalt, open water, dark vegetation, urban, sporadic vegetation and/or bare soil, and mixed water. The training points were acquired virtually by cross referencing high resolution aerial imagery from Google. This model was created in GEE using JavaScript and in Esri's ArcGIS using python scripting, which gave end-users a choice of platform.

The SWIM-ArcMap platform differs from the GEE platform in that the end product is a Boolean sum of the surface water from each indices. The raster bands, like the GEE platform, were used to calculate water indices for further analysis. The training points were then used in a SVM training tool to create classification signatures. The raster classifier then analyzed the signatures and water indices for a classified output. After the bands have been classified, each classification was converted into water vs. non-water and then those bands are combined so that they are given a value of 0-5. A value of 0 indicates the pixel was identified as non-water across all of the classified water indices, while 1 specifies that one of the five classified water indices showed the pixel had water. A value of 2 designates that two of the five classified water indices indicated water and so forth. This gave a degree of confidence for the ArcMap results. For instance, if a pixel was classified as 5 then

there was higher likelihood that surface water was correctly identified for that pixel where a value of 1 meant there was a low confidence water actually existed at that location.

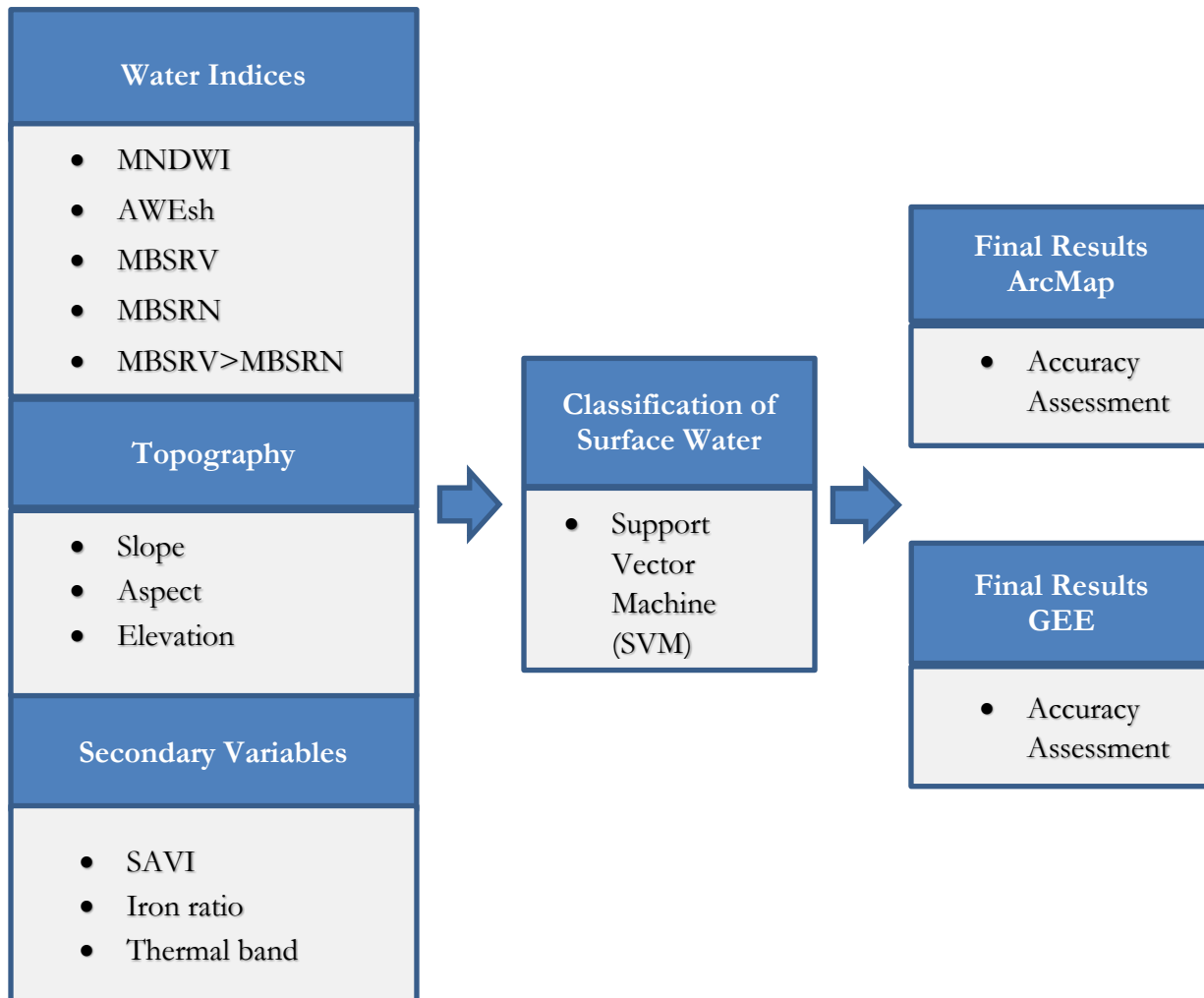


Figure 4 The SWIM tool consisted of three components- water indices (Modification of Normalized Difference Water Index (MNDWI), multi-band spectral relationship near infrared (MBSRN), multi-band spectral relationship visible (MBSRV), Automated Water Extent with Shadow (AWEsh)), topography, and secondary variables (soil adjusted vegetation index (SAVI), the iron ratio, and thermal band 10) derived from Landsat 8 OLI/TIRS imagery and SRTM data. These three components were then added to a classifier within two separate platforms in order to identify surface water bodies, these results then underwent validation.

3.1 Data Acquisition

Two types of data, topography and multi-spectral imagery, were required to develop the SWIM tool. The multi-spectral data were provided by Landsat 8 Operational Land Imager (OLI) surface reflectance (SR) 30 meter spatial resolution data and Thermal Infrared Sensor (TIRS) 100 meter spatial resolution data (U.S. Geological Survey, 2015). The Landsat 8 data were acquired for paths 39 and 38 and rows 30 and 31 during June 9th and 18th 2016. A path refers to how a satellite collects data by running north to south, and a row is the east to west position of each image (Irons, 2016). Each path row combination is an image called a scene. The scenes used in development of SWIM had the least amount of cloud cover and a greater likelihood of surface water collection due to spring snow melt. These Landsat scenes were used from the available repository in GEE and downloaded for use in ArcMap. The topography data came from the Shuttle Radar Topography Mission (SRTM) digital elevation dataset at a 30 meter spatial resolution, which was found in the

GEE repository; or downloaded from the US Department of Agriculture geospatial data gateway for use in ArcMap. Finally, the team visited multiple field sites within the target region and collected *in situ* data for validation.

3.2 Data Processing

3.2.2 Water Indices

The team incorporated water indices into the classification as a means to better locate surface water within the study area. Different types of water indices exist and each have some margin of error. For example, in some instances irrigated croplands may be falsely identified as similar to riparian environment (Donchyts et al. 2016). In order to reduce error, the team used several water indices for the classification. Below is an explanation of water indices that was chosen by the team.

Modification of Normalized Difference Water Index

The modified normalized difference water index (MNDWI) differs from the original normalized difference water index (NDWI) because it is derived from the green and middle short wave infrared (SWIR1) bands rather than the green and near infrared (NIR) bands. The NDWI often overestimates the amount of water due to spectral noise caused by vegetation and soil. The MNDWI is able to remove vegetation, and soil noise while more effectively detecting open water bodies than its alternative, the NDWI (Xu, 2006). Similar to a normal NDWI, the modified NDWI identifies changes in liquid water content of vegetation canopies. MNDWI values range from -1.0 to 1.0, the index maximizes the reflectance values of water and minimizes vegetation and soil values. As water is rarely ever crystal clear, MNDWI is highly sensitive to fluctuations in water quality, but identifies more water spectral signatures than NDWI. However, MNDWI is more vulnerable than NDWI to falsely identify water as shadows caused by hills and clouds (Donchyts et al. 2016). To mitigate these false positive detections of water, the team implemented a supervised classification that examined multiple water indices.

$$A. \quad NDWI = \frac{\rho_{green} - \rho_{NIR}}{\rho_{green} + \rho_{NIR}}$$

$$B. \quad MNDWI = \frac{\rho_{green} - \rho_{SWIR1}}{\rho_{green} + \rho_{SWIR1}}$$

Equations 1 NDWI (A) and MNDWI (B) equation where ρ is the reflectance value of the spectral bands (i.e. green).

Multi-band Spectral Relationships

The multi-band spectral relationship near infrared (MBSRN) is calculated from combining the NIR and SWIR1 bands, while the multi-band spectral relationship visible (MBSRV) is from the green and red bands. The MBSRN band combination was used because these spectral ranges are absorbed by water making the feature darker. When the MBSRV is greater than the MBSRN the pixel is more likely to contain more water than vegetation (Jones & Starbuck, 2015). These calculations result in three of the bands in the SWIM stack.

$$A. \quad MBSRV = \rho_{green} + \rho_{red}$$

$$B. \quad MBSRN = \rho_{NIR} + \rho_{SWIR1}$$

$$C. \quad MBSR_{threshold} = MBSRV > MBSRN$$

Equations 2 Calculations for MBSRV (A), MBSRN (B) and the threshold between the MBSR values (C) where ρ is the reflectance value of the spectral bands (i.e. green).

Automated Water Extent with Shadow (AWE_{sh})

Consisting of the Blue, Green, and SWIR 2 bands, and including MBSRN (Equations 2B), this equation is a further improvement on the distinction of shady areas and dark surfaces. The AWE_{sh} builds upon preexisting

water indices by using a multi-band index rather than relying on dual-band ratios or single-band thresholding. Through band differencing, addition, and applying varying coefficients, the index's primary goal is to maximize separation between water and non-water dark pixels (Feyisa et al. 2014). The application of AWE_{sh} in this study was intended for when shadows present sources of accuracy loss.

$$AWE_{sh} = \rho_{blue} + (2.5\rho_{green}) + (-1.5(\rho_{NIR} + \rho_{SWIR1})) + (-0.25\rho_{SWIR2})$$

Equation 3 Calculation for AWE_{sh} index, where ρ is the reflectance value of the spectral bands (i.e. green)

3.2.3 Topographic variables

A digital elevation model (DEM) from the Shuttle Radar Topography Mission (SRTM) was used in building this model. This particular DEM was chosen to match the 30 meter spatial resolution of the most common Landsat 8 data. In each iteration of SWIM this DEM was used to add layers of elevation, slope, and aspect. A “hillshade” layer was also tested, but found to not add any accuracy to the model. These topography layers add to the ability of SWIM to separate otherwise possible false positives on steep slopes or dry hill faces.

3.2.4 Secondary Variables

Adjusted Vegetation Index (SAVI)

The Normalized Difference Vegetation Index (NDVI) was considered as an indicator of live green vegetation within a pixel as might indicate a water source under the canopy. During testing, the NDVI was found to not add any accuracy to the model. Another vegetation index, however did prove to advance the model: the Soil Adjusted Vegetation Index (SAVI). The SAVI equation builds upon the NDVI equation by introducing a constant to adjust for soil reflectance. That constant can be chosen based on the type of soil to vegetation mixtures one would expect in a given study site from 0 for dense vegetation to 1 for sparse vegetation with more bare soil than green vegetation (Huete, 1988). In this project the constant 0.5 was used to represent an even mixture of bare soil to vegetation. The study area has a large amount of bare soil with sporadic vegetation. Therefore, using this vegetation index did prove to be beneficial.

$$A. \quad NDVI = \frac{\rho_{NIR} - \rho_{red}}{\rho_{NIR} + \rho_{red}}$$

$$B. \quad SAVI = \left(\frac{\rho_{NIR} - \rho_{red}}{\rho_{NIR} + \rho_{red} + L} \right) (1 + L)$$

Equation 4 Calculations for NDVI (A) and for SAVI (B), where ρ is the reflectance value of the spectral bands (i.e. green) and L represents a constant known as the soil brightness correction factor.

Another vegetation index known as Modified Soil Adjusted Vegetation Index (MSAVI2) was also considered during testing but the equation proved to be computationally intensive resulting in runtime errors. When MSAVI2 did run properly the SWIM model took much longer to run, and it did not prove to increase accuracy over the more simple SAVI calculation.

Iron Ratio & Thermal Band

The team found three factors that assisted in distinguishing basalt from water. First, it was important that basalt was distinguished as one of the training classes in the classification process. Second, the thermal signature of basalt is different from water. Therefore, the SWIM model includes one of the thermal bands, band ten, of the Landsat 8 TIRS data. Third, in remote sensing, a ratio of the red band over the green band will assist in distinguishing ferric iron (Kalinowski & Oliver, 2004). Within SWIM, this is referred to as the iron ratio. During testing in GEE the removal of either the thermal band or the iron ratio showed a decrease in accuracy, and a visual difference of water classifications, shown in figure 6, so both were included in the SWIM.

$$\text{ferric iron} = \frac{\rho_{\text{red}}}{\rho_{\text{green}}}$$

Equation 5 Calculation for the iron ratio, where ρ is the reflectance value of the spectral bands (i.e. green)

3.2.5 Agriculture

When choosing land cover type for the classes, it was difficult to determine a class type for agriculture. Crops that were in the process of rotation could have been freshly watered or recently harvested when the Landsat satellite took the image. Watered crops would sometimes be labeled as dark vegetation or mixed water, while dead and dry crops would be mislabeled as urban or bare soil. Mislabeled agricultural regions as water would be inconsequential to land managers who focus on public land. Therefore, it was decided that an agriculture mask would be applied to the final classified map. With the agriculture mask, managers can avoid these areas when looking for natural water regions.

3.3 Data Analysis

3.3.1 Error Matrix

To test the level of accuracy of the classification, an error matrix was used. The classifier was trained with a randomly selected subset of 60 percent of the training points. The error matrix in GEE used the remaining 40 percent of the training points as validation points to compare the class type label to the classification type produced in the map. This process was ran three times with a 60/40 split and a different randomizations each time. The average overall accuracy of the three error matrices was reported in GEE's console. The error analysis process was repeated in ArcMap for comparison. The same 40 percent of random training points were compared with points on the GEE classified map. Once again, three error matrices were produced and then the error matrices produced in ArcMap and GEE were compared to one another.

3.3.2 SWIM results versus the USGS Dynamic Surface Water Extent product (DSWE) and the National Hydrography Dataset (NHD)

The provisional data DSWE products that matched our study area and period were compared with the results from this project. This comparison included the full Landsat scene to maximize the evaluation. Prior to comparison an agriculture mask produced from the 2011 National Land Cover Dataset (NLCD) was applied to the results produced within GEE in such a way that when the two results were compared the mask was also applied to the DSWE results. After this mask was applied, the GEE no water, open water, and mixed water classes were compared to the four classes produced in DSWE, no water, high confidence of water, moderate confidence of water, and partial surface water. The classes for each of these results were generalized so that when a pixel was not classified the same between the two results, areas classified with a high confidence level or said to be partial water were shown as water. The USGS is also responsible for the National Hydrography Dataset (NHD) which was also used to compare with the SWIM results.

4. Results & Discussion

4.1 Analysis of Results

Water Indices

The water indices chosen for the classifier proved to be helpful in distinguishing water within the study area. Choosing just one water index had a higher margin of error for mislabeling. Incorporating the five water indices allowed the classifier to better predict true water. However while having five water indices resulted in better accuracy compared to only one or two water indices, some classes such as mixed water and dark vegetation were still difficult to distinguish. Figure 5 shows the standard deviation for the six classes. The

mixed water and dark vegetation classes had very similar spectral values for all five water index bands, particularly MBSRN and MNDWI. The similar spectral values created difficulty for the classifier when distinguishing between the two classes. Dark vegetation may often be near rivers, ponds, or other mixed water, and adds to the challenge of differentiating the two categories.

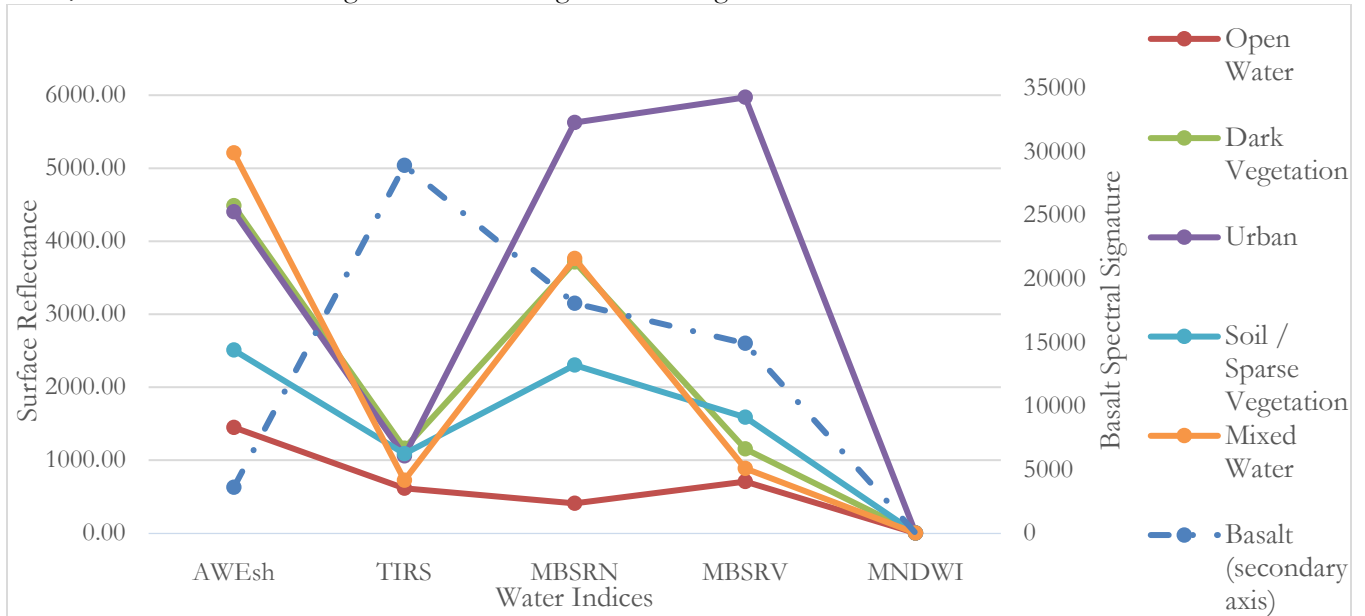


Figure 5 Standard deviation of surface reflectance for the six water indices classes used in SWIM.

Topographic Variables

The study area was located in a hilly and mountainous region, and the spectral signatures of hill shade can be falsely mistaken as water. Hence, incorporating slope, aspect, and elevation into the classifier reduced commission errors arising from these shadows (Jin et al. 2013). Removing any one of these three topographic variables from the GEE model resulted in decreased accuracy of ~2% and removing all three bands decreased accuracy by ~5% when calculating overall accuracy in GEE.

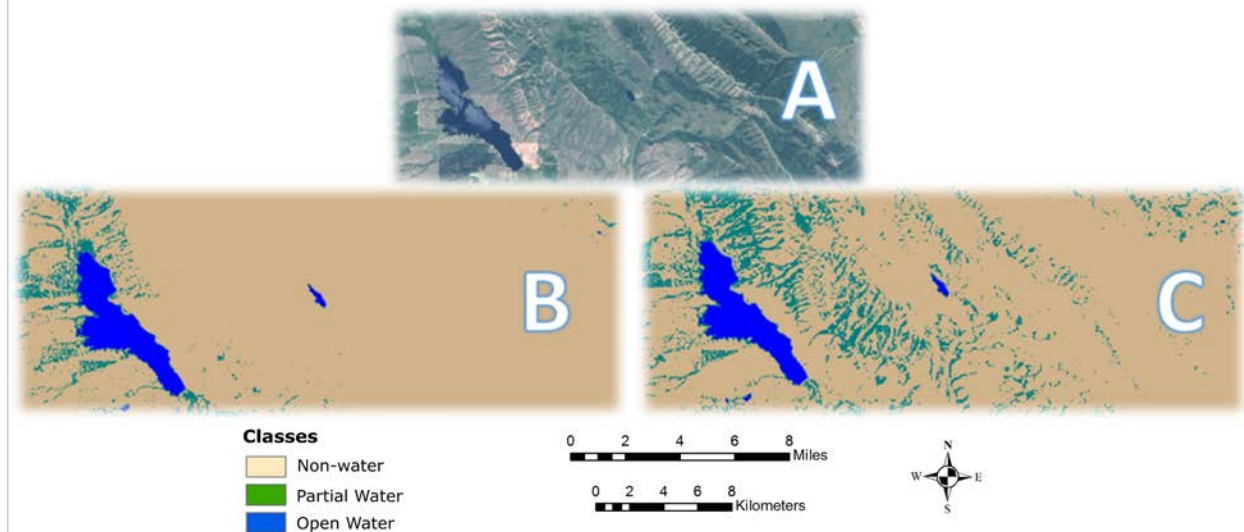


Figure 6 This figure illustrates how topography bands assist in proper classification within SWIM. Figure A shows a Landsat 8 capture within our study area, with Chesterfield reservoir located on the left. Figure B shows the classification of SWIM with open water in blue and mixed water pixels in teal. Figure C shows the over classification that occurs when the topographic layers are removed.

Basalt

Both the thermal band and iron ratio allowed the classifier to better label the basalt regions. Due to the thermal band's coarser resolution of 100 meters, rather than the 30 meters of other Landsat bands, the team tested the classifier with and without the thermal band (Figure 7A-C). Including only the thermal band improved overall accuracy by 4.82% (Figure 7C) and including only the iron ratio improved it by 2.57% (Figure 7B). Including both of these bands improved the overall accuracy by 5.25% and therefore all three bands were included in the model (Figure 8).

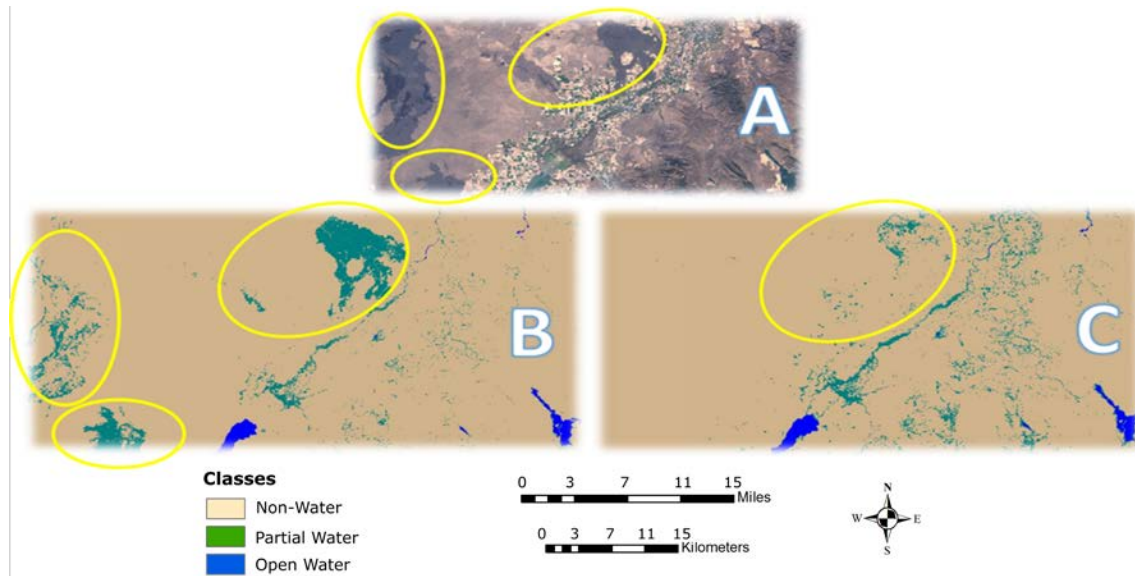


Figure 7 These figures show how basalt was falsely identified as water. Figure A shows the original Landsat 8 scene with Craters of the Moon National Monument on the left. Figure B was classified by the SWIM tool without thermal Band 10, but with the iron ratio. Figure C shows the classified scene without an iron ratio, but with thermal Band 10.

Classifier

After comparing the CART and SVM classifier, the SVM classifier was chosen because the CART overclassified areas of “non-water” as “water”. The SVM processed the data faster and decreased over classification of water, making the classification map more visually intuitive. The CART classifier may have been less intuitive due to the classifier’s preference for categorical inputs, while SVM performed well with continuous data. Due to these benefits the SVM classifier was chosen for the SWIM tool over the CART classifier.

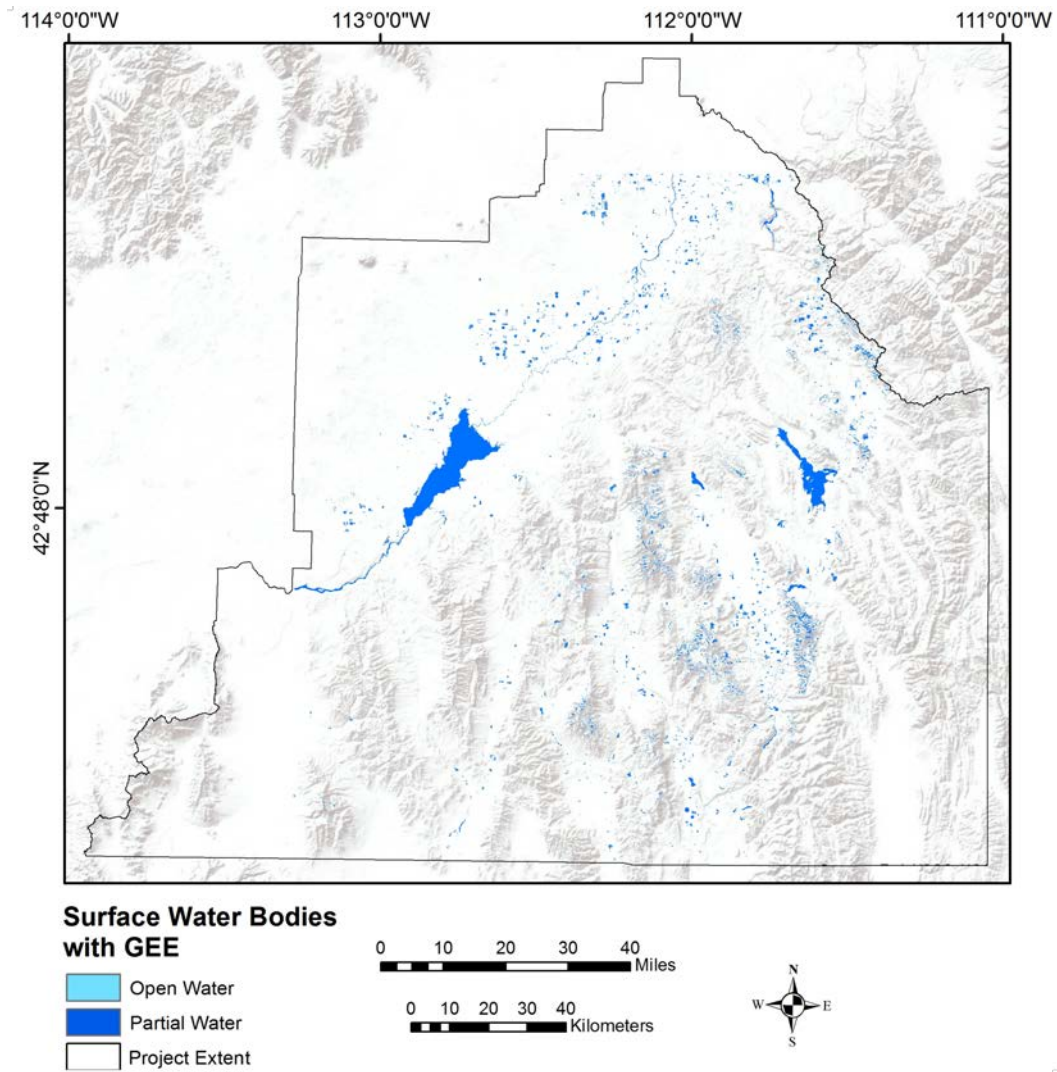


Figure 8 Overview of the study area with the water bodies identified by the SWIM tool while using JavaScript in GEE.

In Figure 9, there still seems to be an over classification of water pixels however, this appears to be mostly due to the partial water classification. This is not surprising, since the class that performed the worst was partial water (Table 1). However, the overall accuracy of the SWIM-GEE platform model was ~ 83%, indicating an accurate model that may only need small adjustments to overcome false identifications of water.

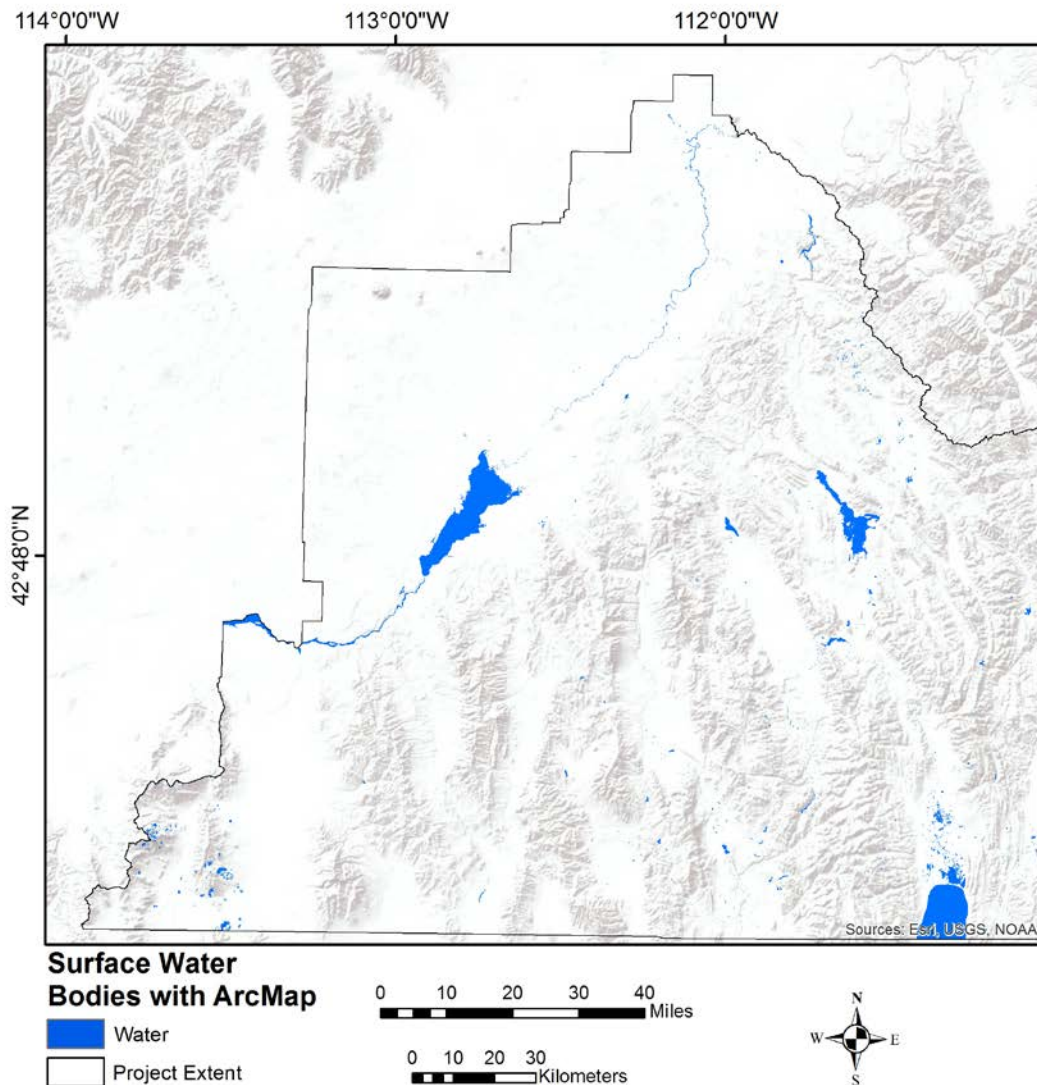


Figure 9 An overview of the study area and the water bodies the SWIM model identified using Python in ArcGIS.

In Figure 9, any pixel that has at least a level two confidence of water is displayed in blue, meaning at least two water indices identified the pixel as water and white is all the pixels with 0 or 1 confidence of water. With just a visual comparison we see the python map matches the GEE map for major water bodies, but some places such as the northern part of the American Reservoir do not show up in python while it showed up in GEE. The overall accuracy of the SWIM-ArcMap platform model was ~ 96%.

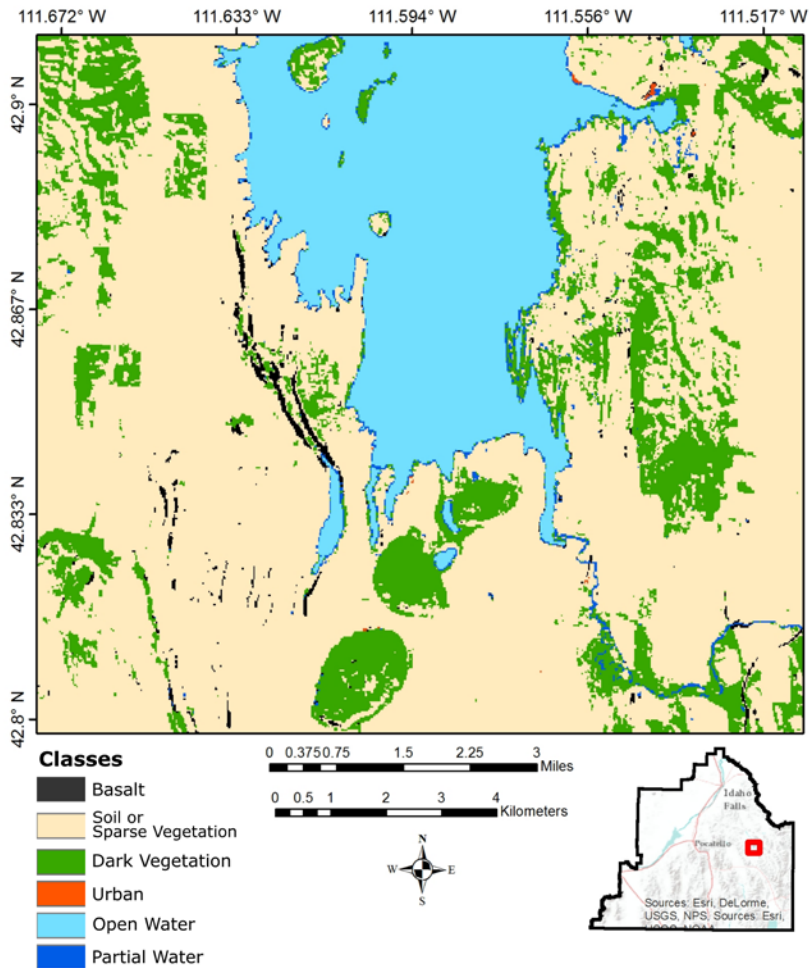


Figure 10 A close up of an area that displays how the SWIM model classifies different features. This is the southern end of Blackfoot reservoir. Most importantly, open water features are clearly defined. Partial water, represented by the stream in the lower right, is still defined, but appears fragmented. The basalt ridges in this area, shown in black, may be mistaken for water in other tools, but are clearly distinguished features when using SWIM.

Error Matrices

When the team initially ran the error matrices in GEE, the software produced an accuracy of 83%. When the same points were used for validation within ArcMap, the overall accuracy for all three matrices was also 83%. Mixed water is the least accurate class and will need further improvement, while open water was one of the best performing classes.

Table 1 Error matrix for overall accuracy of the SWIM tool when using the GEE platform. Each class was verified to determine the likelihood of the model detecting that particular feature. The average accuracy of detecting water was 83%.

Classes	Basalt	Open Water	Dark Vegetation	Urban	Bare Soil/ Sporadic Vegetation	Partial Water	Accuracy
Basalt	147	0	4	1	4	5	92%
Open Water	0	170	0	0	0	2	99%
Dark Vegetation	4	2	155	0	5	11	87%
Urban	13	0	1	127	10	28	71%

Bare Soil / Sporadic Vegetation	4	0	12	11	133	2	82%
Partial Water	8	10	21	17	3	118	67%
Accuracy	83%	94%	81%	81%	86%	71%	83%

Table 2 Error matrix for overall accuracy of the SWIM-GEE when validated within ArcGIS. Individual classes were checked to substantiate the chances of the model identifying that particular feature. Overall accuracy of detecting water was 83%.

Classes	Basalt	Open Water	Dark Vegetation	Urban	Bare Soil/ Sporadic Vegetation	Partial Water	Accuracy
Basalt	147	0	4	1	4	5	92%
Open Water	0	170	0	0	0	2	99%
Dark Vegetation	4	2	155	0	5	11	87%
Urban	13	0	1	127	10	28	71%
Bare Soil / Sporadic Vegetation	4	0	12	11	133	2	82%
Partial Water	8	10	21	17	3	118	67%
Accuracy	83%	94%	81%	81%	86%	71%	83%

Comparison of platform performance of SWIM

When the results from the Earth Engine (Figure 8) and ArcMap (Figure 9) were compared with each other, for the most part, they agreed on the “non-water” class, but there was some variation when it came to where water was located. Most of the disagreement between the ArcMap and GEE platform were due to ArcMap classifying pixels as “non-water” when GEE classified the pixel as “water”. This created a 3.48% of the total 4.95% disagreement (Table 3). This could have been caused by a combination of two things. It may be caused by different platform classification abilities, even though SVM was the chosen classifier in both platforms, each platform may not operate the same. In addition, the last step of the ArcMap platform differs from GEE which may increase pixel filtering of what is considered water. Because most of the disagreement is sourced to when ArcMap classified pixels as “non-water” when GEE classified the pixels as “water”; the cause of disagreement was probably a mix of the two sources. The ArcMap platform itself may not be detecting as much of the partial water compared to the GEE platform. In addition, the last steps in ArcMap which turned everything binary, “water” versus “non-water” rather than attempting to determine whether or not all classes are consistent across each classified imagery, could have resulted in more of the partial water detections becoming filtered out.

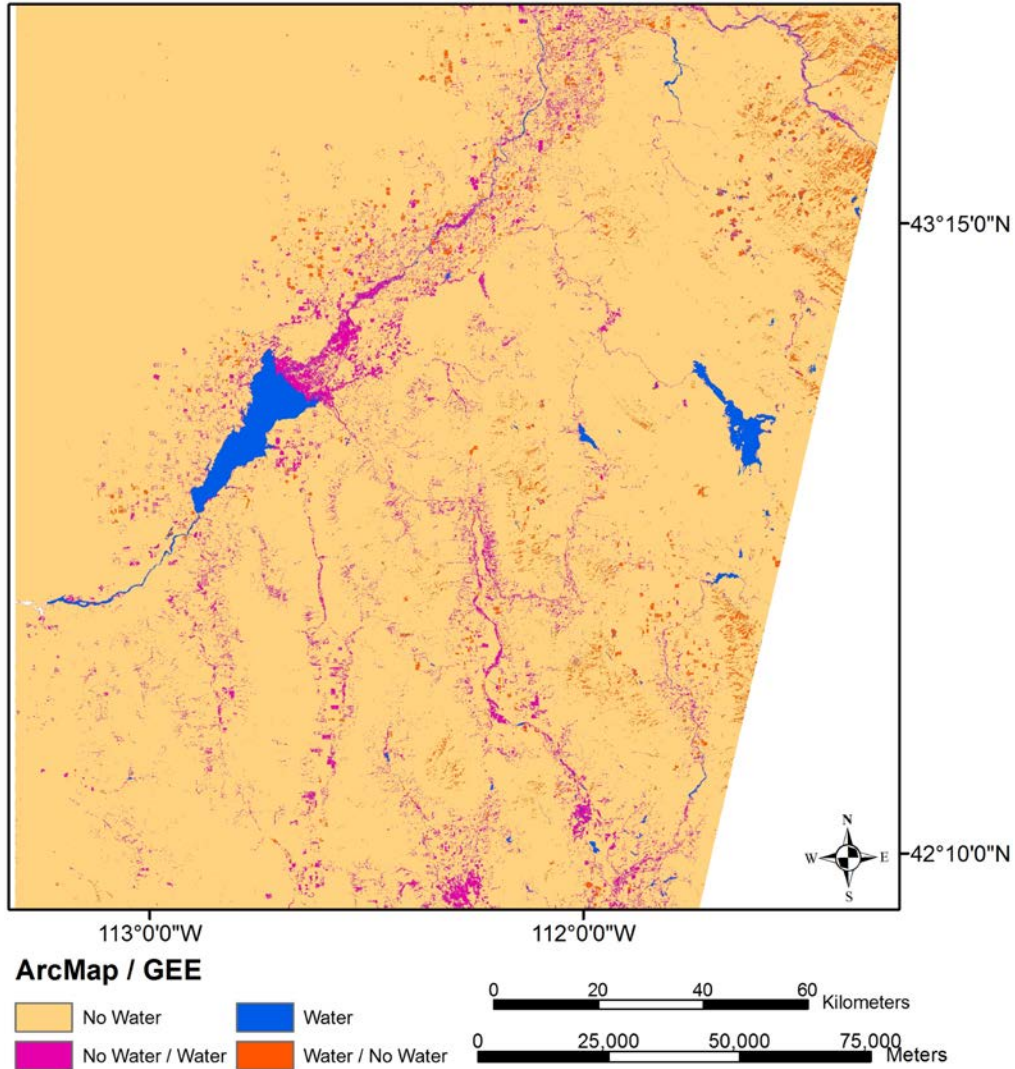


Figure 11 SWIM's results produced in ArcMap were compared to the GEE product. The figure displays pixels that were classified as water (orange) by the ArcMap script and non-water (fuchsia); GEE script classified non-water (orange) and water (fuchsia) pixels; show are areas that both models classified as non-water (gold) and water (blue).

Table 3 Summary of the areas (km^2) compared between SWIM Platforms

	Area	
	KM ²	Percent
Python / GEE		
No Water	2,5095	94%
Water	333	1%
No Water / Water	930	4%
Water / No Water	394	1%
Total Agreement	2,5428	95%
Total Disagreement	1,325	5%

SWIM results versus DSWE and NHD products

As shown in Table 4 most of the 4.99% disagreement between DSWE and SWIM was due to DSWE classifying basalt as water and SWIM classifying non-water as water, where 2.15 % of the 2.54% of the “No Water / Water” comparison is due to partial water classification rather than open water.

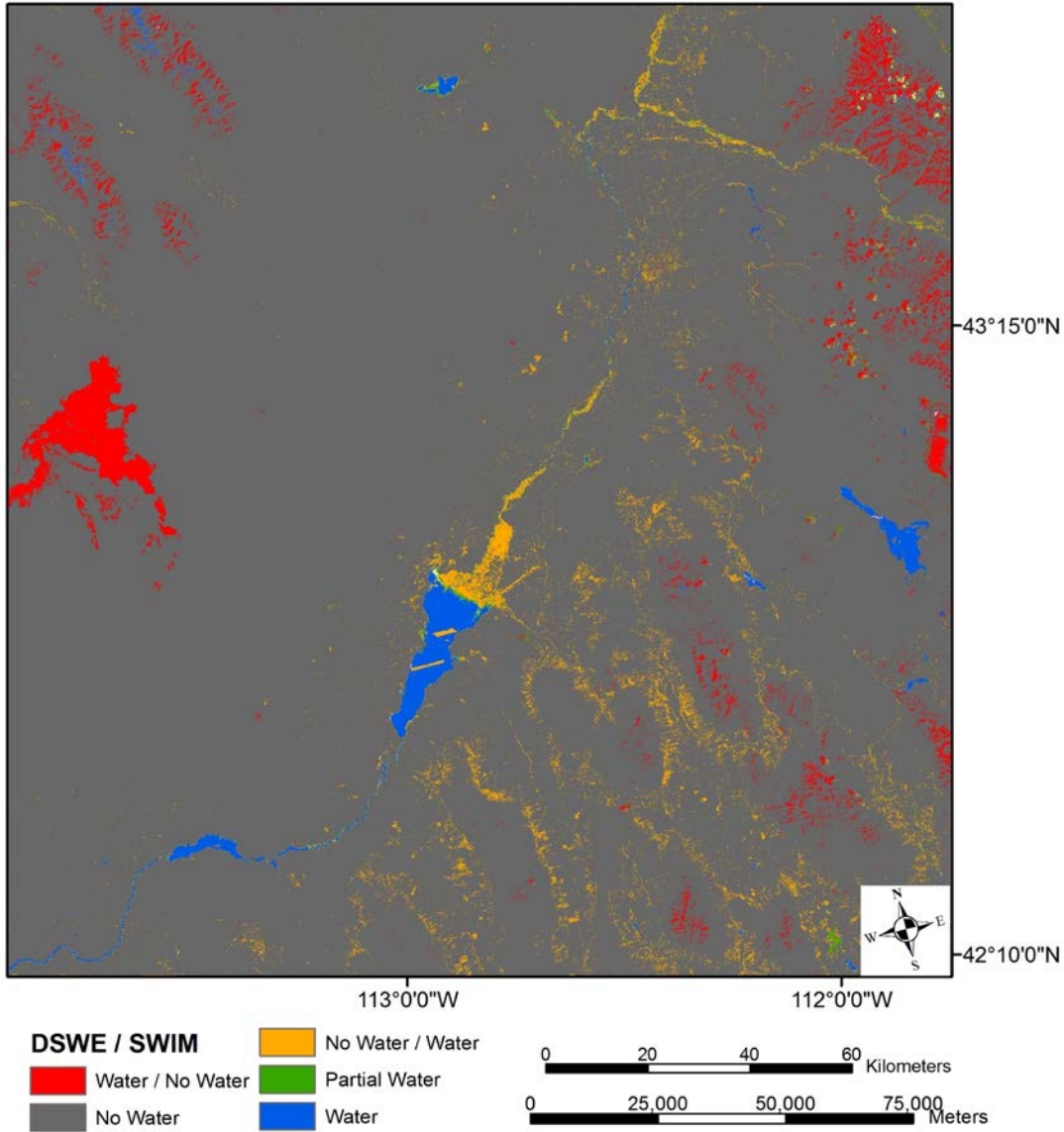


Figure 12 The SWIM results produced using the GEE platform were compared to the DSWE product for the Landsat scene 39/30 (path/row). The figure displays pixels that were classified as water with DSWE and non-water with SWIM (red); pixels that DSWE classified as non-water but SWIM classified as water (orange); and areas that both models classified as non-water (gray), partial water (green), and water (blue).

Table 4 Summary of the areas (km²) compared between DSWE and SWIM classes.

DSWE / SWIM	Area	
	KM ²	Percent
Water / No water	872	2%

No Water / Water	900	3%
Partial Water	75	0%
Water	398	1%
No Water	3,3251	94%
Total Agreement	3,3724	95%
Total Disagreement	1,772	5%

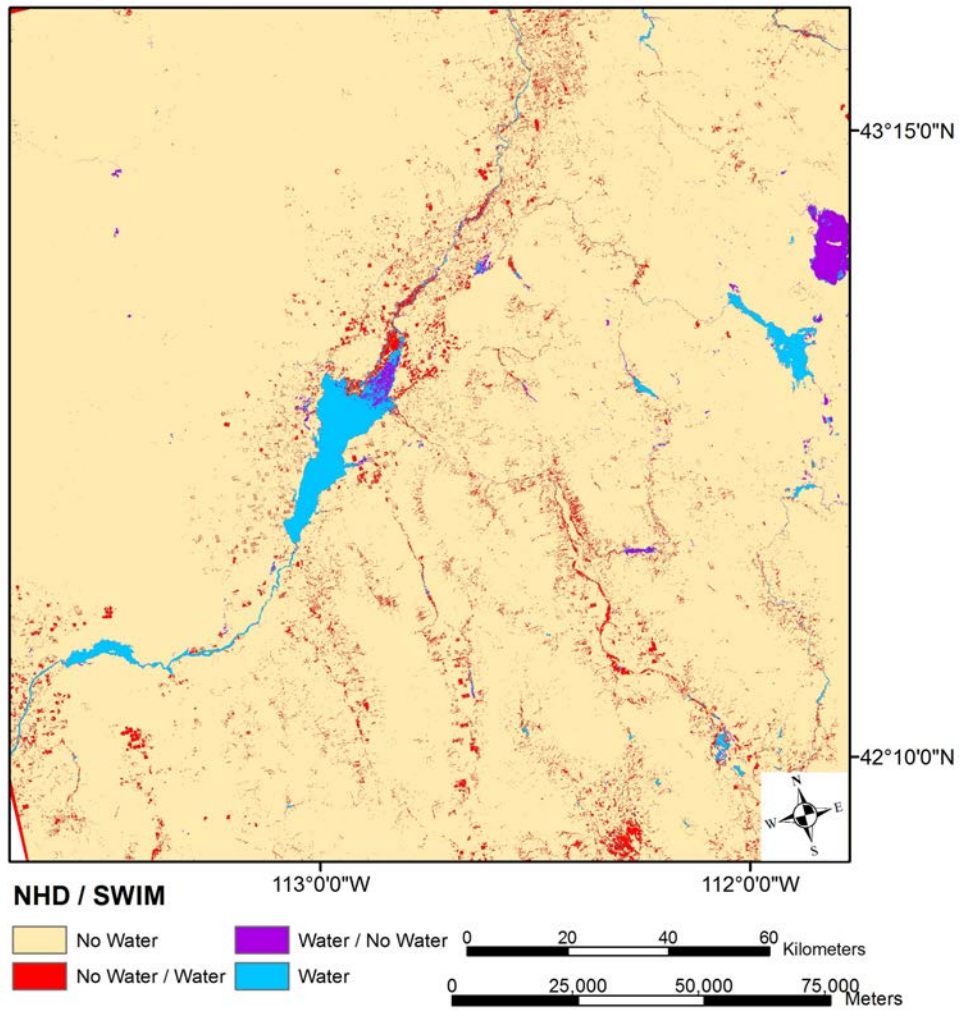


Figure 13 The NHD results produced using the GEE platform were compared to the NHD product for the full project extent. The figure displays pixels that are recorded as water in NHD and non-water with SWIM (purple); pixels that are classified as non-water with NHD and SWIM classified as water (red); and areas that agree between NHD and SWIM for non-water (beige) and water (blue). There may be some discrepancies between the two datasets due to identification of riverine boundaries (blue circle).

The total disagreement, 19.34%, for the NHD-SWIM comparison is the highest seen out of the three comparisons performed in this project. This disagreement does have founding when visual checks are completed on areas NHD has identified as water and SWIM does not (purple of Figure 13). However, some of the disagreements could be explained with differences in boundaries. For instance, the NHD does have a riparian area identified in its database (blue circle Figure 13), however, it is shown in red in Figure 13. This is, most likely because SWIM identified a greater boundary than the boundary recorded in NHD.

Table 5 Summary of the areas (km^2) compared between NHD and SWIM classes.

NHD / SWIM	Area	
	Square kilometer	Percentage
No Water	34,053	79%
No Water / Water	8,162	19%
Water / No Water	201	0%
Water	820	2%
Total Agreeance	34,873	81%
Total Disagreement	8,363	19%

4.2 Future Work

Model Alteration

Future studies will use the methods developed in the first term to discern between intermediate and perennial surface water areas, while excluding ephemeral bodies, and enhancing tool development. The current results detected disjointed river networks, this problem may be fixed by employing additional variables and/or introducing new methods for boundary detection. For instance, a path-tracking algorithm can be applied to the pixels which indicates the likelihood of a pixel belonging to a linear feature, it then connects those pixels. This would aid in decreasing fragmentation. In addition, other thresholds may be necessary to eliminate falsely identified partial water pixels which will hopefully increase model performance for partial water classification.

Multiple scenes

This project tested the SWIM tool on one scene. For the next term, the team wants to test the SWIM tool on another temporal scene to test the model's effectiveness. The scenes originally chosen were in early June and contained few clouds. Other scenes may have more clouds, meaning the SWIM tool may need to incorporate a cloud mask. Colder seasons such as fall and winter will have more snow cover which may disrupt detection of water resources since water reflection signatures may not pierce snow cover. In addition to snow, water presence in the region may vary due to seasonality. Scenes from other seasons may identify more regions with water bodies that dry up by June. In addition, some of the water bodies that remained in June, contained murky water from sediment deposition which may be falsely classified as mixed water or bare soil. Changes in sediment deposition can also be due to seasonality, for example spring may have less sediment due to the melting of snow. Comprehending how seasonality affects the models will further improve water management.

5. Conclusions

A Surface Water Indication Model was built inside GEE, while an analogous script was constructed in ArcMap. A Support Vector Machine (SVM) classified the water indices, topographic data, and secondary variables. The water indices were comprised of the AWEsh, MNDWI, SAVI, MBSRV, MBSRN, and iron ratio equations, as well as the thermal band "B10", which derived from Landsat 8 Operational Land Imager (OLI), Thermal Infrared Sensor (TIRS). Topographic information, consisting of slope, aspect, and elevation, was extracted from the Shuttle Radar Topography Mission (SRTM). The SVM was trained with over 400 training points per class to produce six: basalt, open water, dark vegetation, urban, sporadic vegetation/bare

soil, and mixed water. Leveraging several water indices, instead of just one, enabled the classifier to better predict and identify water. Error matrices validated the overall accuracy of 83% for identifying water. However, distinguishing between the mixed water and dark vegetation classes proved difficult for the classifier. An agriculture mask was used to eliminate watered crops that would sometimes be labeled as dark vegetation or mixed water. The GEE and ArcMap scripts were compared against each other, where overall python performance was better than GEE performance. However, python results lost partial water information and gained a confidence indicator. In addition, the DSWE product was compared to the GEE results. DSWE consistently identified basalt as open water and did a better job of refining the partial water classification. This may indicate that SWIM's performance could be better improved by including thresholds within the model.

6. Acknowledgments

A special thank you to our contributors for their time and assistance with this project

- Advisors: Keith Weber, Lead Science Advisor (GIS Training and Research Center at Idaho State University); Charles Peterson (Biology Department, Idaho State University); Mark Carroll (NASA GSFC)
- Project Partners: Karen Kraus, Bureau of Land Management (BLM), Range Technician; Michele Mavor, Bureau of Land Management (BLM), Fire Ecologist; Linda Davis, Idaho Department of Water Resources (IDWR), Senior GIS Analyst; Danielle Bruno-Fayreau, Idaho Department of Water Resources (IDWR), GIS Analyst
- Others: Kelly Meehan, NOAA National Centers for Environmental Health, Geoinformatics Fellow; David Thau, Google, Senior Developer Google Earth Engine

Any opinions, findings, and conclusions or recommendations expressed in this material are those of the author(s) and do not necessarily reflect the views of the National Aeronautics and Space Administration.

This material is based upon work supported by NASA through contract NNL11AA00B and cooperative agreement NNX14AB60A.

7. References

- Bauer, M. E., Biehl L. L., Robinson B. F. (1980) Final Report Volume 1: Field Research on the Spectral Properties of Crops and Soils. NASA Rep. SR-PO-O4022. Laboratory for Applications of Remote Sensing. West Lafayette, IN.
- Berk. (2009, November 6). Classification and Regression Trees. Data Mining with Rattle and R: The Art of Excavating Data for Knowledge Discovery. *Use R*, pp. 36-350. Retrieved from <http://doi.org/10.1007/s00038-011-0315-z>
- Breiman, L., Friedman, J., Stone, C. J., & Olshen, R. A. (1984). Classification and regression trees. CRC press.
- Burges, C. J. C. (1998). A Tutorial on Support Vector Machines for Pattern Recognition. *Data Mining and Knowledge Discovery*, 2(2), 121–167. <http://doi.org/10.1023/A:1009715923555>
- Cafarella, M., Chang, E., Fikes, A., Halevy, A., Hsieh, W., Lerner, A., Madhavan, J., Muthukrishnan, S. (2008). Data management projects at Google. *ACM SIGMOD Record*, 37(1), 34–38. <http://doi.org/10.1145/1374780.1374789>
- Cortes, C., Vapnik V. (1995, March 8). Support Vector Networks. *Machine Learning*. Retrieved from <http://link.springer.com/10.1007/BF00994018>

- Donchyts, G., Schellekens, J., Winsemius, H., Eisemann, E., & Van de Giesen, N. (2016). A 30 m Resolution Surface Water Mask Including Estimation of Positional and Thematic Differences Using Landsat 8, SRTM and OpenStreetMap: A Case Study in the Murray-Darling Basin, Australia. *Remote Sensing*, 8, 386. Retrieved from <http://doi.org/10.3390/rs8050386>
- Feyisa, G. L., Meilby, H., Fensholt, R., & Proud, S. R. (2014). Remote Sensing of Environment Automated Water Extraction Index : A new technique for surface water mapping using Landsat imagery. *Remote Sensing of Environment*, 140, 23-35.
- Irons, James R. (2016, November). The Worldwide Reference System. NASA. Retrieved from <http://landsat.gsfc.nasa.gov/the-worldwide-reference-system/>
- Jawak, Jawak, S. D., Kulkarni, K., & Luis, A. J. (2015). A Review on Extraction of Lakes from Remotely Sensed Optical Satellite Data with a Special Focus on Cryospheric Lakes. *Advances in Remote Sensing*, 04(03), 196–213. Retrieved from <http://doi.org/10.4236/ars.2015.43016>
- Jin, S., Homer, C., Yang, L., Xian, G., Fry, J., Danielson, P., & Townsend, P. A. (2013). Automated cloud and shadow detection and filling using two-date Landsat imagery in the USA. *International Journal of Remote Sensing*, 34(5), 1540–1560. Retrieved from <http://doi.org/10.1080/01431161.2012.720045>
- Jones, J. W., & Starbuck, M. J. (2015, April 10). *USGS.gov*. Retrieved from Dynamic Surface Water Extent (DSWE): http://remotesensing.usgs.gov/ecv/document/dswe_algorithm_description.pdf
- McFeeters, S. K. (2013). Using the Normalized Difference Water Index (NDWI) within a Geographic Information System to Detect Swimming Pools for Mosquito Abatement: A Practical Approach. *Remote Sensing*, 5(7), 3544-3561. Retrieved from <http://doi.org/10.3390/rs5073544>
- Saraswat, M. (2016, April 12). A Complete Tutorial on Tree Based Modeling from Scratch (in R & Python). Retrieved from <https://www.analyticsvidhya.com/blog/2016/04/complete-tutorial-tree-based-modeling-scratch-in-python/>
- U.S. Fish and Wildlife Service. (2002). *National wetlands inventory: A strategy for the 21st century*. Washington, DC: U.S. Department of the Interior, Fish and Wildlife Service.
- U.S. Geological Survey (2015, January). Landsat 8 OLI (Operational Land Imager) and TIRS (Thermal Infrared Sensor) | The Long Term Archive. Retrieved from <https://lta.cr.usgs.gov/L8>
- Wright, C., & Gallant, A. (2007). Improved wetland remote sensing in Yellowstone National Park using classification trees to combine TM imagery and ancillary environmental data. *Remote Sensing of Environment*, 107, 582-605.
- Xu, H. (2006). Modification of Normalized Difference Water Index (NDWI) to Enhance Open Water Features in Remotely Sensed Imagery. *International Journal of Remote Sensing*, 27(14), 3025-3033. Retrieved from <http://doi.org/10.1080/01431160600589179>

8. Content Innovation

Content Innovation #1

Audio Slides

Emailed to Tiffani.N.Miller@nasa.gov with filename

2016Fall_ID_SoutheasternIdahoWaterResources_AudioSlides

OR shared through Google Drive at: https://drive.google.com/file/d/0B_TuQyq-v3XaYmZOMmVZeU9DNTg/view?usp=sharing

Content Innovation #2

Featured Multimedia (VPS video)

shared through Google Drive at:

<https://drive.google.com/drive/folders/0B1hph8rGPOhFcUxmOC1uemZ5MXM>

Content Innovation #3

Inline Supplementary Material

TABLE 1 ERROR MATRIX FOR OVERALL ACCURACY OF THE SWIM TOOL WHEN USING THE GEE PLATFORM. EACH CLASS WAS VERIFIED TO DETERMINE THE LIKELIHOOD OF THE MODEL DETECTING THAT PARTICULAR FEATURE. THE AVERAGE ACCURACY OF DETECTING WATER WAS 91%.....	14
TABLE 2 ERROR MATRIX FOR OVERALL ACCURACY OF THE SWIM-GEE WHEN VALIDATED WITHIN ARCGIS. INDIVIDUAL CLASSES WERE CHECKED TO SUBSTANTIATE THE CHANCES OF THE MODEL IDENTIFYING THAT PARTICULAR FEATURE. OVERALL ACCURACY OF DETECTING WATER WAS 87%.....	15
TABLE 3 SUMMARY OF THE AREAS (KM ²) COMPARED BETWEEN SWIM PLATFORMS.....	16
TABLE 4 SUMMARY OF THE AREAS (KM ²) COMPARED BETWEEN DSWE AND SWIM CLASSES.	17
TABLE 5 SUMMARY OF THE AREAS (KM ²) COMPARED BETWEEN NHD AND SWIM CLASSES.	19
EQUATIONS 1 NDWI (A) AND MNDWI (B) EQUATION WHERE P IS THE REFLECTANCE VALUE OF THE SPECTRAL BANDS (I.E. GREEN)	7
EQUATIONS 2 CALCULATIONS FOR MBSRV (A), MBSRN (B) AND THE THRESHOLD BETWEEN THE MBSR VALUES (C) WHERE P IS THE REFLECTANCE VALUE OF THE SPECTRAL BANDS (I.E. GREEN).	7
EQUATION 3 CALCULATION FOR AWE _{SH} INDEX, WHERE P IS THE REFLECTANCE VALUE OF THE SPECTRAL BANDS (I.E. GREEN)	8
EQUATION 4 CALCULATIONS FOR NDVI (A) AND FOR SAVI (B), WHERE P IS THE REFLECTANCE VALUE OF THE SPECTRAL BANDS (I.E. GREEN) AND L REPRESENTS A CONSTANT KNOWN AS THE SOIL BRIGHTNESS CORRECTION FACTOR.	8
EQUATION 5 CALCULATION FOR THE IRON RATIO, WHERE P IS THE REFLECTANCE VALUE OF THE SPECTRAL BANDS (I.E. GREEN)	9
FIGURE 1 STUDY AREA EXTENT (RED) OF SOUTHEASTERN IDAHO WATER RESOURCES PROJECT... 2	
FIGURE 2 CLASSIFYING WITH SVM WHERE TWO CLASSES (SHOWN AS CIRCLES FOR WATER AND SQUARES FOR NON-WATER) ARE KNOWN TO BE PRESENT. A) THE MEAN IS SHOWN WITH THE LINE AND HAS BEEN TRICK OPTIMIZED SO THAT THE DISTANCES FROM THE CLOSEST POINT IN EACH OF THE TWO GROUPS WILL BE FARTHEST AWAY. WHEREVER THE UNLABELED SIGNATURES FALL WILL DECIDE IF IT IS WATER OR NOT WATER. B) WHEN THE LABELED TRAINING DATA HAS TOO MUCH VARIATION A TRANSFORMATION IS IMPLEMENTED AND A HYPERPLANE (SHOWN IN BLUE) IS CREATED.....	3

FIGURE 3 A VISUALIZATION OF CART DECISION TREE.	4
FIGURE 4 THE SWIM TOOL CONSISTED OF THREE COMPONENTS- WATER INDICES (MODIFICATION OF NORMALIZED DIFFERENCE WATER INDEX (MNDWI), MULTI-BAND SPECTRAL RELATIONSHIP NEAR INFRARED (MBSRN), MULTI-BAND SPECTRAL RELATIONSHIP VISIBLE (MBSRV), AUTOMATED WATER EXTENT WITH SHADOW (AWESH)), TOPOGRAPHY, AND SECONDARY VARIABLES (SOIL ADJUSTED VEGETATION INDEX (SAVI), THE IRON RATIO, AND THERMAL BAND 10) DERIVED FROM LANDSAT 8 OLI/TIRS IMAGERY AND SRTM DATA. THESE THREE COMPONENTS WERE THEN ADDED TO A CLASSIFIER WITHIN TWO SEPARATE PLATFORMS IN ORDER TO IDENTIFY SURFACE WATER BODIES, THESE RESULTS THEN UNDERWENT VALIDATION.....	6
FIGURE 5 STANDARD DEVIATION OF SURFACE REFLECTANCE FOR THE SIX WATER INDICES CLASSES USED IN SWIM.....	10
FIGURE 6 THESE IMAGES ILLUSTRATE HOW TOPOGRAPHY BANDS ASSIST IN PROPER CLASSIFICATION WITHIN SWIM. IMAGE A SHOWS A LANDSAT 8 CAPTURE WITHIN OUR STUDY AREA, CHESTERFIELD RESERVOIR, ON THE LEFT. IMAGE B SHOWS THE CLASSIFICATION OF SWIM WITH OPEN WATER IN BLUE AND MIXED WATER PIXELS IN TEAL. IMAGE C SHOWS THE OVER CLASSIFICATION THAT OCCURS WHEN THE TOPOGRAPHIC LAYERS ARE REMOVED. ..	10
FIGURE 7 THESE IMAGES SHOW HOW BASALT WAS FALSELY IDENTIFIED AS WATER. IMAGE A SHOWS THE ORIGINAL LANDSAT 8 SCENE WITH CRATERS OF THE MOON NATIONAL MONUMENT ON THE LEFT. IMAGE B WAS CLASSIFIED BY THE SWIM MODEL WITHOUT THERMAL BAND 10, BUT WITH THE IRON RATIO. IMAGE C SHOWS THE CLASSIFIED SCENE WITHOUT AN IRON RATIO, BUT WITH THERMAL BAND 10. IN THE CLASSIFICATIONS OPEN WATER IS BLUE AND MIXED WATER IS TEAL.....	11
FIGURE 8 OVERVIEW OF THE STUDY AREA WITH THE WATER BODIES IDENTIFIED BY THE SWIM TOOL WHILE USING JAVASCRIPT IN GEE.	12
FIGURE 9 AN OVERVIEW OF THE STUDY AREA AND THE WATER BODIES THE SWIM MODEL IDENTIFIED USING PYTHON IN ARCGIS.....	13
FIGURE 10 A CLOSE UP OF AN AREA THAT DISPLAYS HOW THE SWIM MODEL CLASSIFIES DIFFERENT FEATURES. THIS IS THE SOUTHERN END OF BLACKFOOT RESERVOIR. MOST IMPORTANTLY, OPEN WATER FEATURES ARE CLEARLY DEFINED. PARTIAL WATER, REPRESENTED BY THE STREAM IN THE LOWER RIGHT, IS STILL DEFINED, BUT APPEARS FRAGMENTED. THE BASALT RIDGES IN THIS AREA, SHOWN IN BLACK, MAY BE MISTAKEN FOR WATER IN OTHER TOOLS, BUT ARE CLEARLY DISTINGUISHED FEATURES WHEN USING SWIM.	14
FIGURE 11 SWIM'S RESULTS PRODUCED IN ARCMAP WERE COMPARED TO THE GEE PRODUCT. THE FIGURE DISPLAYS PIXELS THAT WERE CLASSIFIED AS WATER (ORANGE) BY THE ARCMAP SCRIPT AND NON-WATER (FUCHSIA); GEE SCRIPT CLASSIFIED NON-WATER (ORANGE) AND WATER (FUCHSIA) PIXELS; SHOW ARE AREAS THAT BOTH MODELS CLASSIFIED AS NON- WATER (GOLD) AND WATER (BLUE).....	16
FIGURE 12 THE SWIM RESULTS PRODUCED USING THE GEE PLATFORM WERE COMPARED TO THE DSWE PRODUCT FOR THE LANDSAT SCENE 39/30 (PATH/ROW). THE FIGURE DISPLAYS PIXELS THAT WERE CLASSIFIED AS WATER WITH DSWE AND NON-WATER WITH SWIM (RED); PIXELS THAT DSWE CLASSIFIED AS NON-WATER BUT SWIM CLASSIFIED AS WATER (ORANGE); AND AREAS THAT BOTH MODELS CLASSIFIED AS NON-WATER (GRAY), PARTIAL WATER (GREEN), AND WATER (BLUE).	17
FIGURE 13 THE NHD RESULTS PRODUCED USING THE GEE PLATFORM WERE COMPARED TO THE NHD PRODUCT FOR THE FULL PROJECT EXTENT. THE FIGURE DISPLAYS PIXELS THAT ARE RECORDED AS WATER IN NHD AND NON-WATER WITH SWIM (PURPLE); PIXELS THAT ARE CLASSIFIED AS NON-WATER WITH NHD AND SWIM CLASSIFIED AS WATER (RED); AND AREAS	

THAT AGREE BETWEEN NHD AND SWIM FOR NON-WATER (BEIGE) AND WATER (BLUE).
THERE MAY BE SOME DISCREPANCIES BETWEEN THE TWO DATASETS DUE TO
IDENTIFICATION OF RIVERINE BOUNDARIES (BLUE CIRCLE)..... 18

9. Appendices

Table 6 Error Matrix for the first out of three classifications completed and accuracy calculated in GEE.

Classes	Basalt	Open Water	Dark Vegetation	Urban	Bare Soil/ Sporadic Vegetation	Mixed Water	Accuracy
Basalt	159	0	2	0	3	10	91%
Open Water	0	190	0	0	0	4	98%
Dark Vegetation	5	2	151	0	6	12	86%
Urban	9	0	1	117	8	41	66%
Bare Soil / Sporadic Vegetation	2	0	10	15	135	4	81%
Mixed Water	12	1	14	10	1	132	78%
Accuracy	85%	98%	85%	82%	88%	65%	84%

Table 7 Error Matrix for the second out of three classifications completed and accuracy calculated in GEE.

Classes	Basalt	Open Water	Dark Vegetation	Urban	Bare Soil/ Sporadic Vegetation	Mixed Water	Accuracy
Basalt	141	0	3	3	1	2	94%
Open Water	0	159	0	0	0	1	99%
Dark Vegetation	6	2	156	1	6	5	89%
Urban	11	0	0	137	18	9	78%
Bare Soil / Sporadic Vegetation	8	0	14	3	130	0	84%
Mixed Water	6	21	23	24	6	97	55%
Accuracy	82%	87%	80%	82%	81%	85%	83%

Table 8 Error Matrix for the third out of three classifications completed and accuracy calculated in GEE.

Classes	Basalt	Open Water	Dark Vegetation	Urban	Bare Soil/ Sporadic Vegetation	Mixed Water	Accuracy
Basalt	141	0	7	0	7	2	90%
Open Water	0	161	0	0	0	2	99%
Dark Vegetation	2	1	157	0	4	16	87%
Urban	19	0	1	128	4	35	68%
Bare Soil / Sporadic Vegetation	2	1	11	16	135	3	80%

Mixed Water	6	7	26	18	2	124	68%
Accuracy	83%	95%	78%	79%	89%	68%	82%

Table 9 Error Matrix for the first out of three classifications completed in GEE and accuracy calculated in ArcMap.

Classes	Basalt	Open Water	Dark Vegetation	Urban	Bare Soil/ Sporadic Vegetation	Mixed Water	Accuracy
Basalt	159	0	2	0	3	10	91%
Open Water	0	190	0	0	0	4	98%
Dark Vegetation	5	2	151	0	6	12	86%
Urban	9	0	1	117	8	41	66%
Bare Soil / Sporadic Vegetation	2	0	10	15	135	4	81%
Mixed Water	12	1	14	10	1	132	78%
Accuracy	85%	98%	85%	82%	88%	65%	84%

Table 10 Error Matrix for the second out of three classifications completed in GEE and accuracy calculated in ArcMap.

Classes	Basalt	Open Water	Dark Vegetation	Urban	Bare Soil/ Sporadic Vegetation	Mixed Water	Accuracy
Basalt	141	0	3	3	1	2	94%
Open Water	0	159	0	0	0	1	99%
Dark Vegetation	6	2	156	1	6	5	89%
Urban	11	0	0	137	18	9	78%
Bare Soil / Sporadic Vegetation	8	0	14	3	130	0	84%
Mixed Water	6	21	23	24	6	97	55%
Accuracy	82%	87%	80%	82%	81%	85%	83%

Table 11 Error Matrix for the third out of three classifications completed in GEE and accuracy calculated in ArcMap.

Classes	Basalt	Open Water	Dark Vegetation	Urban	Bare Soil/ Sporadic Vegetation	Mixed Water	Accuracy
Basalt	141	0	7	0	7	2	90%
Open Water	0	161	0	0	0	2	99%
Dark Vegetation	2	1	157	0	4	16	87%
Urban	19	0	1	128	4	35	68%
Bare Soil / Sporadic Vegetation	2	1	11	16	135	3	80%
Mixed Water	6	7	26	18	2	124	68%
Accuracy	83%	95%	78%	79%	89%	68%	82%